Twentieth-century warming and the dendroclimatology of declining yellow-cedar forests in southeastern Alaska

Colin M. Beier, Scott E. Sink, Paul E. Hennon, David V. D'Amore, and Glenn P. Juday

Abstract: Decline of yellow-cedar (*Chamaecyparis nootkatensis* ((D. Don) Spach) has occurred on 200 000 ha of temperate rainforests across southeastern Alaska. Because declining forests appeared soon after the Little Ice Age and are limited mostly to low elevations (whereas higher elevation forests remain healthy), recent studies have hypothesized a climatic mechanism involving early dehardening, reduced snowpack, and freezing injury. This hypothesis assumes that a specific suite of microclimatic conditions occurs during late winter and declining cedar populations across the region have responded similarly to these conditions. Based on the first geographically extensive tree ring chronologies constructed for southeastern Alaska, we tested these assumptions by investigating regional climatic trends and the growth responses of declining cedar populations to this climatic variation. Warming winter trends were observed for southeastern Alaska, resulting in potentially injurious conditions for yellow-cedar due to reduced snowfall and frequent occurrence of severe thaw–freeze events. Declining cedar forests shared a common regional chronology for which late-winter weather was the best predictor of annual growth of surviving trees. Overall, our findings verify the influence of elevational gradients of temperature and snow cover on exposure to climatic stressors, support the climatic hypothesis across large spatial and temporal scales, and suggest cedar decline may expand with continued warming.

Résumé : Le dépérissement du chamaecyparis jaune (*Chamaecyparis nootkatensis* (D. Don) Spach) s'étend sur une superficie de 200 000 ha de forêt humide tempérée partout dans le sud-est de l'Alaska. Parce que le dépérissement des forêts est apparu peu de temps après le Petit Âge glaciaire et qu'il est surtout limité aux forêts situées à faible altitude, alors que les forêts situées aux altitudes plus élevées demeurent en santé, des études récentes ont posé l'hypothèse d'un mécanisme climatique impliquant un désendurcissement hâtif, une faible accumulation de neige et des dommages dus au gel. Cette hypothèse suppose qu'une suite spécifique de conditions microclimatiques survient à la fin de l'hiver et que les populations de chamaecyparis jaune qui dépérissent partout dans la région ont réagi de la même façon à ces conditions. Sur la base de données dendrochronologiques couvrant pour la première fois un vaste territoire dans le sud-est de l'Alaska, nous avons testé ces hypothèses en étudiant les tendances climatiques régionales et les réactions en croissance des populations dépérissantes de chamaecyparis jaune à ces changements climatiques. Des tendances au réchauffement pendant l'hiver ont été observées dans le sud-est de l'Alaska, engendrant possiblement des conditions qui pourraient endommager le chamaecyparis jaune à cause de la diminution des chutes de neige et de l'occurrence répétée d'épisodes sévères de dégel suivi de gel. Les forêts de chamaecyparis jaune qui dépérissent ont une chronologie régionale commune pour laquelle les conditions de fin d'hiver prédisaient le mieux la croissance annuelle des arbres qui survivent. Dans l'ensemble, nos résultats confirment l'influence des gradients de température à la hausse et du couvert nival sur l'exposition à des facteurs de stress climatiques, supportent l'hypothèse du climat à grande échelle dans le temps et l'espace et indiquent que le dépérissement du chamaecyparis jaune pourrait s'intensifier avec la progression du réchauffement.

[Traduit par la Rédaction]

Introduction

Yellow-cedar (*Chamaecyparis nootkatensis* ((D. Don) Spach), also known as Alaska-cedar or yellow-cypress, is a long-lived, slow-growing tree species of high ecological, commercial, and cultural importance in southeastern Alaska. The species has an extensive natural range from northern California to Prince William Sound in south-central Alaska.

Received 21 August 2007. Accepted 28 November 2007. Published on the NRC Research Press Web site at cjfr.nrc.ca on 26 April 2008.

C.M. Beier.[1,2] Department of Biology and Wildlife, University of Alaska Fairbanks, Fairbanks, AK 99775-7000, USA.
S.E. Sink and G.P. Juday. School of Natural Resources and Agricultural Sciences, University of Alaska Fairbanks, Fairbanks, AK 99775-7200, USA.
P.E. Hennon and D.V. D'Amore. USDA Forest Service, Pacific Northwest Research Station, Forestry Sciences Laboratory, Juneau, AK 99801, USA.

[1]Corresponding author (e-mail: cbeier@esf.edu).
[2]Present address: College of Environmental Science and Forestry, State University of New York, 1 Forestry Drive, Syracuse, NY 13210-2778, USA.

 doi:10.1139/X07-240

In Alaska, yellow-cedar can be found from near timberline to sea level, whereas populations further south tend to be limited to high-elevation sites (Harris 1990). Extant populations in southeastern Alaska probably originated from early Holocene northward migration along the Pacific Northwest coast, as well as from smaller unglaciated refugia in the region (Carrarra et al. 2003). The cool-moist climate of the late Holocene (4500 years B.P.) favored the establishment and expansion of yellow-cedar in southeastern Alaska, especially on sites with poor soil drainage (Hebda 1983). Beginning more recently (500 years B.P.) in the late Holocene, a period of overall cooling trends (with occasional warm periods) known as the Little Ice Age (LIA) persisted in the region until about 1880 (Heusser et al. 1985); during the LIA, coastal glaciers in southeastern Alaska advanced, reached their contemporary maximums in the late 19th century, and have since been retreating rapidly (Viens 2001).

Dieback of yellow-cedar forests was first observed in southeastern Alaska in 1909 and was recently found in the northernmost coastal areas of British Columbia (Hennon et al. 2005). Stand age studies suggest that declining cedar populations were established during the LIA and that the onset of decline occurred between 1880 and 1900 (Hennon and Shaw 1994), roughly coinciding with the end of the LIA in southeastern Alaska. Dead and dying yellow-cedar have been observed on over 200 000 ha in southeastern Alaska (Wittwer 2004), mostly at elevations below 300 m. Declining stands contain snags in various stages of decay, suggesting that several pulses of mortality have occurred during the 20th century. Decline pathology is indicated by foliar browning and rapid death, followed by tree death occurring after 3–15 years; in declining stands, all age and size classes have been affected by dieback (Hennon and Shaw 1997). A comprehensive body of research (see Hennon et al. 2006) on the pathology of cedar decline has effectively ruled out biotic mechanisms (e.g., higher fungi, oomycetes, insects, nematodes, viruses, mycoplasmas, and bears) and suggested an abiotic, climatic mechanism (Hennon and Shaw 1997).

Relative to other endemic conifers, the dehardening process for yellow-cedar is highly temperature dependent (Puttonen and Arnott 1994; Hawkins et al. 2001). Thus, the species may be prone to early dehardening when triggered by thaw conditions in the late-winter months (Schaberg et al. 2005, 2008). Most declining stands are found in open-canopy forests on poorly drained sites, whereas cedar remains healthy on similar sites at higher elevations (Hennon and Shaw 1997). Open-canopy cedar forests experience greater extremes in diurnal variation of ground-level air and upper-horizon soil temperatures than closed-canopy forests. Snow cover effectively insulates these forest soils from temperature extremes, including hard freezes common in the late-winter climate of southeastern Alaska (D'Amore and Hennon 2006). However, in the absence of adequate snow cover, yellow-cedar may be especially vulnerable to soil freezing because of shallow rooting in saturated soils (Hennon and Shaw 1994; Hennon et al. 2006). In general, spring freezing injury to conifers tends to be more severe on warm slopes and (or) at low elevations (Havranek and Tranquillini 1995). Both factors are consistent with cedar decline, which is almost entirely found at low elevations, and more commonly on south- and west-facing slopes, especially in the northern areas of decline (Wittwer 2004). Belowground injury, indicated by extensive mortality of fine roots in the upper soil horizon, appears to be the trigger for the appearance of decline symptoms in the crowns of affected trees (Hennon and Shaw 1997). New experimental findings indicate that dehardened yellow-cedar is highly vulnerable to root freezing if simulated snow is removed prior to frost. Potted yellow-cedar saplings growing outdoors in Juneau during a typical thaw–freeze cycle (in 2006) that received this "snow removal" treatment experienced 100% mortality by the end of spring (Schaberg et al. 2008).

In sum, these observations helped generate our current working hypothesis of yellow-cedar decline, which posits that belowground freezing injury is the proximate cause of fine root mortality and subsequent crown death (Hennon and Shaw 1997; Hennon et al. 2006). Cedar populations at high elevations and in northern areas of southeastern Alaska are thought to remain healthy because of a lower frequency and (or) magnitude of thaw conditions, and deeper and (or) more persistent snowpack that insulates soils (and shallow root systems) from freezing. Although there are observational studies (Hennon and Shaw 1994; Schaberg et al. 2005; D'Amore and Hennon 2006) and recent experimental findings (Schaberg et al. 2008) that support this mechanism, it is founded on several assumptions about events at larger scales that remain unproven: (*i*) currently declining cedar forests were established during the relatively colder climate of the LIA; (*ii*) climatic changes during the 20th century have resulted in a suite of conditions that have become injurious to low-elevation cedar populations; and (*iii*) all declining cedar populations have responded similarly to these climatic conditions.

Evaluating these assumptions is necessary because our climatic mechanism presumes that historical changes have caused cedar dieback in previously healthy populations. In other words, we sought to confirm that our working hypothesis was well founded in the context of broader scale changes in southeastern Alaska that have been poorly documented until now. Current knowledge suggests the regional climate has been warming more slowly than other mesoscale climates in the circumpolar north (Viens 2001; ACRC 2007). However, because the maritime climate of southeastern Alaska exhibits a relatively narrow range of temperatures throughout the year (for northern latitude regions), smaller changes in mean temperatures may have significant consequences, especially on winter precipitation and snowfall. We are unaware of existing research that has described trends and (or) outcomes of 20th century climate change in southeastern Alaska, including shifts in local weather phenomena and their impacts on the phenology and health of old-growth temperate rainforests. More specifically, there is uncertainty whether the conditions dictated by our hypothesis, i.e., thaw–freeze cycles occurring during winters where snow cover is inadequate to insulate low elevation forest soils, have occurred with sufficient frequency and severity to result in widespread yellow-cedar mortality in southeastern Alaska.

To address these issues at the appropriate spatial and temporal scales, we compiled historical climate data sets based on instrumental records and constructed regionally extensive tree-ring chronologies for declining and healthy yellow-cedar populations. To our knowledge, both the climate and tree-ring data sets are the first of their kind for the region of southeastern Alaska (but see Laroque and Smith 1999; Viens 2001). With these data, we (*i*) analyzed the impacts of recent climatic change on winter temperature and precipitation conditions; (*ii*) estimated the frequency and magnitude of potentially injurious winter thaw–freeze events; (*iii*) described the relative importance and influence of late-winter climate on yellow-cedar growth; and (*iv*) compared yellow-cedar growth and climatic responses among declining and healthy populations. We synthesized these findings to evaluate larger scale changes in climate and cedar growth in southeastern Alaska and, given the validity of our assumptions, to provide landscape-scale inferences on the relationship between climate change and yellow-cedar decline during the 20th century.

Methods

Study area

The southeastern region of Alaska extends from Icy Bay near Yakutat (59°N,140°W) to Dixon Entrance (55°N, 130°W) and includes the western portions of the Coast Range on the mainland and the Alexander Archipelago. Modern climate is mild and hypermaritime with abundant year-round precipitation, no prolonged dry periods, and comparatively milder seasonal conditions (i.e., cooler summers and warmer winters) than continental climates at similar latitudes. Mean annual rainfall is approximately 2500 mm and ranges from approximately 1300 mm in the north (Haines) to nearly 4000 mm in the south (Ketchikan). Vegetation is overwhelmingly conifer-dominated, including coastal spruce–hemlock forests, muskegs (peat bogs), alpine dry tundra, and some areas of deciduous forest and shrubs (Viereck and Little 1986). In general, forest productivity is governed by gradients in soil drainage dictated by slope, parent material, and peat accumulation. Along a productivity gradient, vegetation ranges from large stature closed-canopy forests on well-drained soils to stunted open-canopy forest and shrub bogs or muskegs on saturated peat soils (Neiland 1971). High rainfall supports a coastal rainforest dominated by western hemlock (*Tsuga heterophylla* (Raf.) Sarg.) and Sitka spruce (*Picea sitchensis* (Bong.) Carr.) with smaller amounts of mountain hemlock (*Tsuga mertensiana* (Bong.) Carr.), shore pine (*Pinus contorta* Dougl. ex Loud. var. *contorta*), western redcedar (*Thuja plicata* Donn), and yellow-cedar. Mountain hemlock and yellow-cedar are abundant at treeline; yellow-cedar is also common on poorly drained sites at low elevations, where declining stands are common (Hennon et al. 1990).

Climate data preparation and analysis

Instrumental climate records used in this study included daily minimum and maximum temperature, precipitation, and snowfall for six weather stations (see Fig. 1). All weather stations were located near sea level (from 3 to 35 m elevation), met First Order standards by 1950, and have semicontinuous records dating back to 1910 or earlier. Significant gaps occur in the data, ranging from several days to years in length, and weather stations have had changes in location and data collection methods since installation. Mean daily (MDT) and mean monthly temperature (MMT) were compiled from daily minimum–maximum records. MMT values were not calculated from MDT data if the monthly record contained a gap of more than three consecutive days, or 5 days total. MMT gaps were filled using the average difference method (Vincent and Gullett 1999) based on the closest available station; if none existed within 20 km, the MMT gap was not filled. For temporal extension of instrumental records in the Sitka and Ketchikan areas, we joined records from pairs of stations in close proximity (e.g., Japonski Island and Magnetic Observatory for Sitka; Ketchikan airport and Annette Island for Ketchikan) using a method described by Juday (1984). Both station pairs met the criterion for joining records (see Vincent and Gullett 1999) with respect to homogeneity of variance, although the Ketchikan–Annette pair did not meet the criterion for proximity (i.e., within a few kilometres), because the two stations were located about 18 km apart. Subsequent analyses using weather records focused on the Sitka, Ketchikan-Annette, Petersburg, and Wrangell records. We decided to exclude Juneau weather records, because strong local variation in climate confounded our attempts to combine the two station records (as we did for Ketchikan–Annette and Sitka). In Juneau, the downtown station is located in a narrow and steep fjord-like channel, and the airport station is located 8 miles north in an open wetland adjacent to the Mendenhall Glacier. Although downtown weather is consistently wetter, the lack of a consistent correlation in MDT between the stations prevented aggregation of records. We note that this issue was not relevant to the Juneau tree-ring sample population, which was located 20 miles north of the airport station.

Simple linear regression models were used to identify significant trends in late-winter MMT (January–April), late-winter total monthly precipitation (MPPT) (January–April), and total winter snowfall in the Sitka, Ketchikan–Annette, Petersburg, and Wrangell records. In the complex, dissected and mountainous terrain of southeastern Alaska, snow deposition and accumulation varies with landscape position, elevation, and circulation patterns. Because we lacked spatially explicit data sets of historical snow accumulation, we aggregated local records into a regional mean of annual snowfall (October–April) from 1950 to 2004; these data were normalized for use in estimation of thaw–freeze impact, as described in the following section.

Thaw–freeze events

Thaw–freeze events were evaluated as potential stressors by their frequency and magnitude during the 20th century. Mean daily temperature was used to estimate the number of growing days (MDT ≥ 5 °C) and freezing days (MDT ≤ 0 °C) for each year, from the period of 1 February through 1 May, for the four localities with the best daily records (e.g., Ketchikan–Annette, Sitka, Petersburg, and Wrangell). We chose 1 February as the starting date, because recent findings suggest it is the earliest that yellow-cedar may begin dehardening under ambient thaw conditions (Schaberg et al. 2005, 2008) and because severe foliar injury to yellow-cedar saplings commonly occurs during March and

April (P.E. Hennon, unpublished data). The ending date was chosen because hard frosts were not found in instrumental records after 1 May. Growing days (GD) and freezing days (FD) were used to identify potential thaw–freeze events in the weather records. The thresholds of duration of thawing (for dehardening) and freezing (for injury) for yellow-cedar remain unresolved, so we based our thaw–freeze criteria on a literature review (Sperry and Sullivan 1992; Puttonen and Arnott 1994; Auclair et al. 1996; Laroque and Smith 1999; Hawkins et al. 2001; Bourque et al. 2005). From this research, we decided to use two criteria to query the daily records: (*i*) at least three growing days followed by at least one freezing day, hereafter abbreviated as 3GD, 1FD events, and (*ii*) at least seven growing days followed by at least three freezing days, or 7GD, 3FD events. These sample sets approximated thaw–freeze frequency using an upper bound (the 3GD, 1FD subset) and a lower bound (the 7GD, 3FD subset). Lastly, to determine the regional extent of thaw–freeze events, we recorded the proportion of available stations where an event was found, e.g., three of four stations, one of three stations.

The magnitude of thaw–freeze events was estimated by an index combining (*i*) thaw intensity prior to frost and (*ii*) freezing intensity after the thaw. To estimate thaw intensity, growing degree-days (GDD) were calculated by the cumulative degrees ≥5 °C MDT from 1 February to the last freezing day of the winter. To estimate freezing intensity, cooling degree-days (CDD) were calculated by the cumulative degrees ≤0 °C MDT from the end of a thaw until the last freezing day of the winter. Thaw–freeze magnitude was estimated by summing GDD and CDD for each weather record in each year where a 3GD, 1FD thaw–freeze event was observed. In the infrequent cases when multiple thaw–freeze events occurred in a single record during the same winter, this method provided an aggregated estimate of thaw–freeze magnitude. Because of data limitations, largely related to the location of weather stations near sea level, these analyses did not account for influences of elevation or aspect on air temperature or precipitation that would be relevant at the local (i.e., stand-level) scale.

Lastly, because snow cover is central to our working hypothesis of cedar decline, we estimated the relative impact of thaw–freeze events by calculating an index based on (*i*) our estimates of thaw–freeze magnitude and (*ii*) a proxy for snow cover. For the snow cover proxy, we normalized mean annual snowfall based on the 54 year mean of available records (1950–2004), using the subtraction method (i.e., [observed – mean]/SD). We then combined the estimate of thaw–freeze magnitude with the proxy of winter snow cover, to provide a composite index of potential thaw–freeze impact:

$$[1] \qquad I = M_{\mathrm{tf}} \times \mathrm{SC}_t$$

where I is the estimated impact of thaw–freeze event, M_{tf} is the thaw–freeze magnitude (mean GDD + mean CDD), and SC_t is the snow cover (average snowfall in year t normalized by 1950–2004 mean).

Because snowfall measurements were not recorded consistently in southeastern Alaska prior to 1950, our estimates of potential impact were limited to the period of 1950–2004. We ranked all years from 1950–2004 to identify the most potentially significant thaw–freeze events in the weather records. In developing this index, we made the assumption that greater snowfall results in deeper snow cover that, in turn, reduces the likelihood of soil freezing associated with cedar injury and mortality. Therefore, based on this index, a strong thaw–freeze event during a high snowfall year is posited to have a lesser impact than a weaker thaw–freeze event during a low snowfall year.

Tree ring series and standardized chronologies

We located sampling areas using digitized maps of observed cedar decline and the existing road network. Most of our sites were below 300 m elevation and within 10 km of a road; we did not sample within 100 m of the road corridor, downhill of clearcuts, or within 100 m of clearcut edges. We attempted a wide regional dispersion of sites within four provinces: Peril Strait, Central islands, northern and southern Prince of Wales Island (Fig. 1). The sample population included 17 declining populations and two healthy populations; healthy stands were located at Poison Cove Bog and Juneau (Table 1). The Juneau site was the only population located outside of the observed geographic range of cedar decline, i.e., where low-elevation yellow-cedar remains healthy. In the Peril Strait province, we sampled two stands in the same watershed (Poison Cove): a low-elevation declining stand (Poison Cove Decline) and a high-elevation healthy stand (Poison Cove Bog) located at approximately 30 and 240 m elevation, respectively. We intended that paired sites at Poison Cove would provide a "space for time" model in which the modern high-elevation site would have a similar microclimate, with respect to temperatures (air and soil) and snow cover (depth and persistence), to the low-elevation site during the putatively colder period of the LIA. Both sites are southwest facing and have similar slope and soil profiles. Poison Cove sampling also provided a context for interpreting chronologies using measurements of air–soil microclimate at these sites (D'Amore and Hennon 2006).

Increment coring was conducted at approximately breast height on a minimum of 15 live yellow-cedar trees chosen randomly at each site. We obtained at least two ring series per tree, either by coring completely through the bole (from the bark through pith to bark opposite) or with multiple single (bark to pith) radial cores. Ring series were visually cross-dated with a dissecting microscope and measured to 0.001 mm resolution using a Velmex sliding stage apparatus. Analysis of tree ring data requires several preliminary steps: cross-dating, detrending (standardization), and normalization. COFECHA software was used to detect potential cross-dating errors in ring series (Holmes 1983). Dating errors were corrected, and series with apparent missing rings were excluded from the analysis, i.e., of the 312 trees sampled, 254 were used (81.4%). For all trees with two or more accurately cross-dated series, we used the mean width of each ring in the analysis.

Ring series were detrended and converted into standardized chronologies using ARSTAN software (Cook and Krusic 2005). We used the interactive detrending option of ARSTAN to examine each ring series and determine if detrending was needed. The most common detrending option applied in tree ring studies is the negative exponential

Fig. 1. Maps of observed cedar decline, sample sites, weather stations, and sampling provinces in southeastern Alaska. Cedar decline map based on aerial surveys (Wittwer 2004). All weather stations meet First Order standards and are located near sea level.

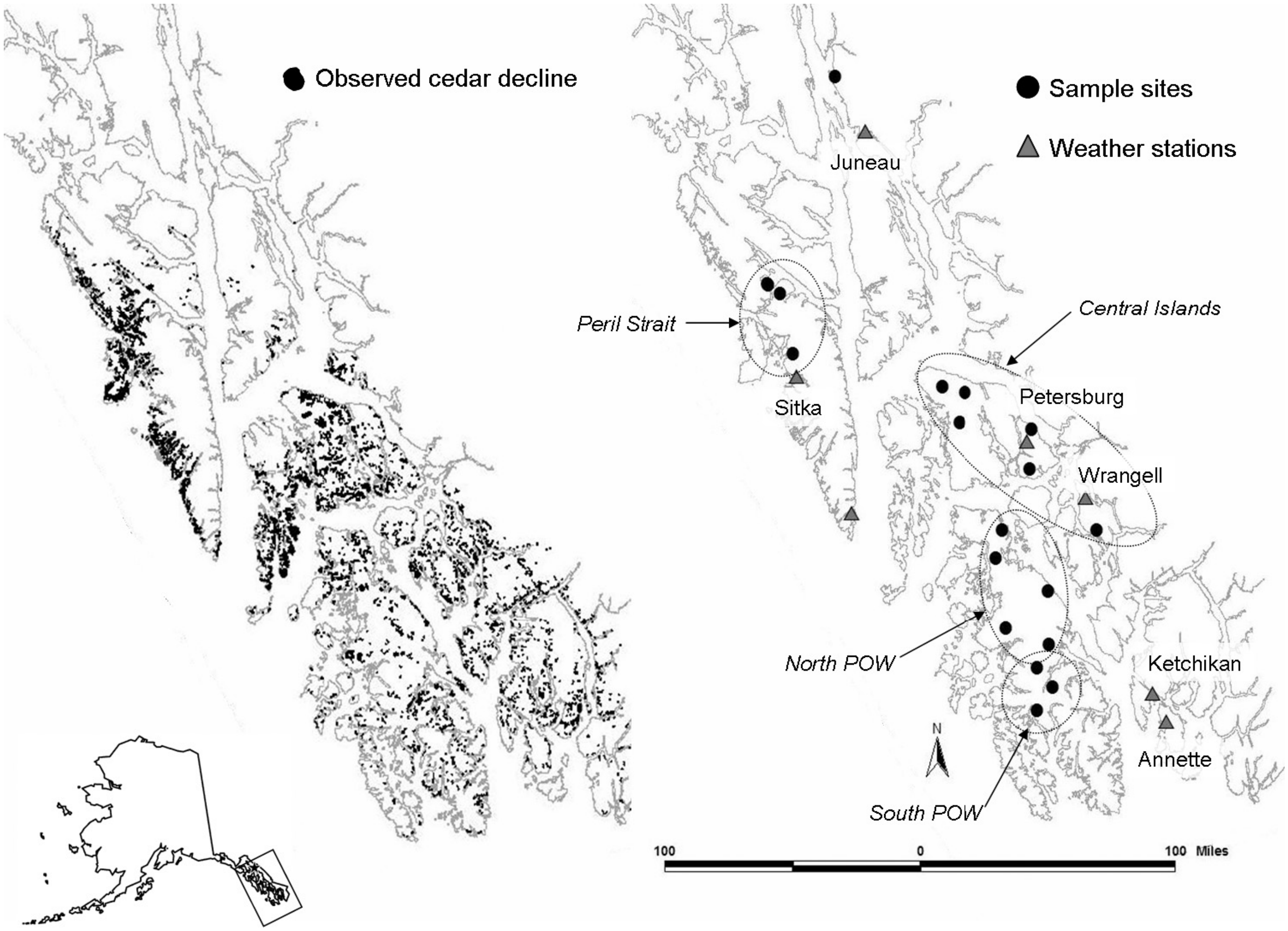

Table 1. Sites, sample size, and regional groupings for aggregation of site chronologies.

Chronology	No. of sites	No. of trees
Total	19	254
Declining populations	17	227
Prince of Wales Island (POW)	8	90
Northern POW	5	57
Southern POW	3	33
Central Islands	6	72
Mitkof	2	26
Kupreanof	3	31
Nemo (Wrangell)	1	15
Peril Strait	3	65
Poison Cove	2	51
Sitka	1	14
Healthy populations	2	27
Poison Cove Bog	1	12
Juneau	1	15

function that accounts for the geometric bias in early radial growth of the bole. Because most of the trees sampled were over 300 years old and our window of interest was from 1800 to 2004, geometric bias was quite low, and the detrending procedure minimally altered most series. After detrending, ARSTAN was used to generate standardized chronologies, from which we directly derived annual ring-width indices (RWI) for each series. Ring series for each tree were aggregated (by site) into mean site chronologies, and the mean site RWI were normalized using the subtraction method ([observed – mean]/SD) for 1800–2004. Overall, these steps produced mean site RWI for statistical analysis. Mean site RWI were then aggregated by averaging sites within provinces (see Table 1), and mean province RWI were compared in correlation matrices to determine the presence (and strength) of common growth patterns among declining and healthy populations. For paired sites in the Poison Cove watershed, we stratified this analysis by century, to compare growth patterns prior to the onset of decline (i.e., during the LIA) and during the ongoing decline phenomenon (i.e., since the end of the LIA).

Climate–growth analyses

Growth responses of cedar populations to climatic variation during the 20th century were determined using regression and correlation analyses. Multivariate linear models were used to identify baseline climate influences, i.e., the

Table 2. Estimated late-winter warming trends in southeastern Alaska during the 20th century, based on linear regression parameters.

	Mean monthly temperature trends (°C/100 years)			
	January	February	March	April
Ketchikan–Annette	2.81***	2.91***	2.26***	2.24***
Wrangell–Petersburg	0.18	1.5*	1.3*	0.66
Sitka	0.17	–0.26	–0.57	–0.44

Note: Asterisks indicate model significance:*, $p < 0.05$; ***, $p < 0.0001$.

Fig. 2. Winter temperature trends in southeastern Alaska during the 20th century based on simple linear regression models of Ketchikan–Annette combined records. Light dotted lines are 95% confidence intervals.

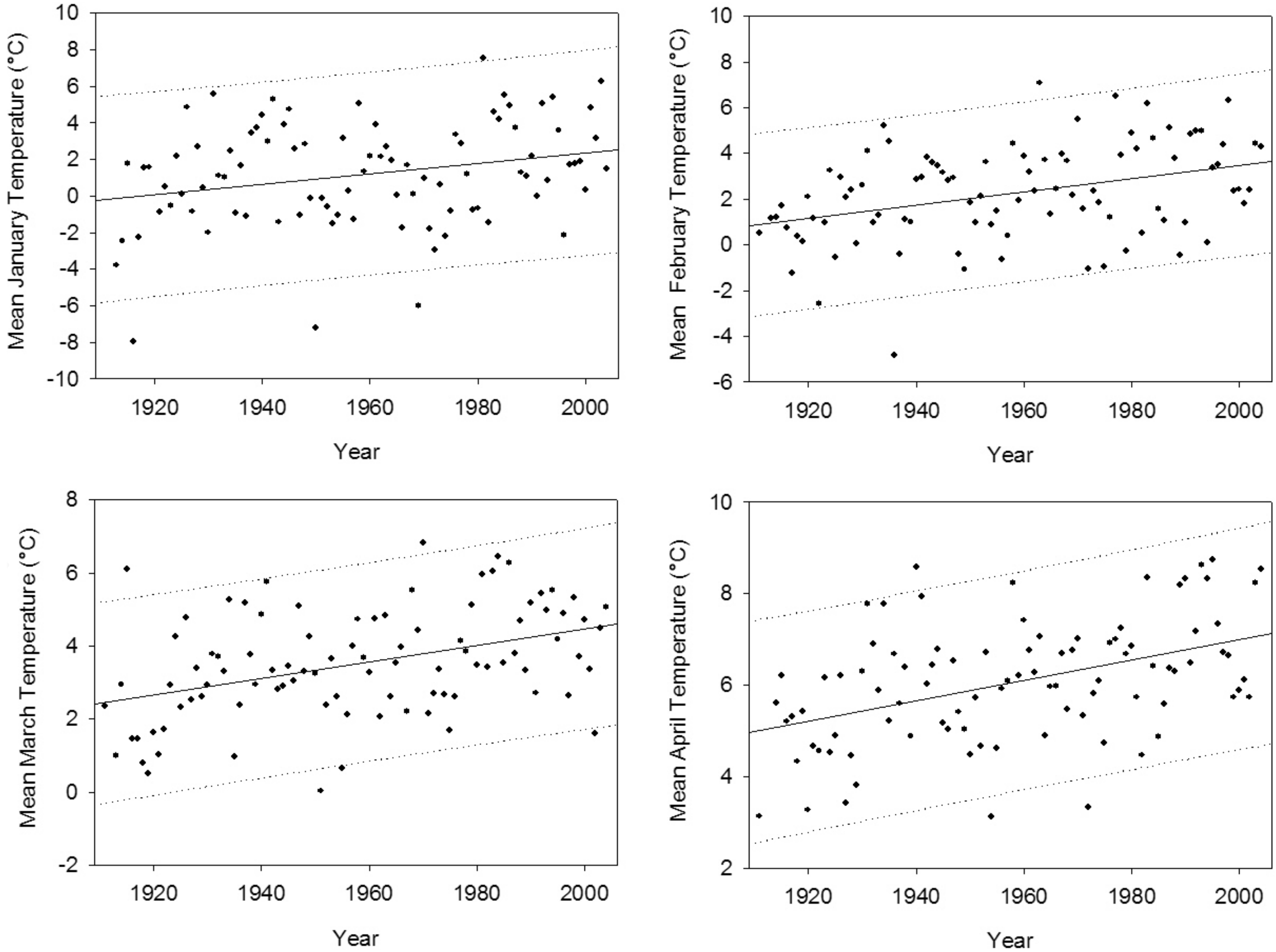

monthly indices of temperature and precipitation that best explained interannual variation in historical cedar growth. Models applied a stepwise regression procedure with MMT and MPPT indices as explanatory variables, and yellow-cedar regional RWI values as the response variables. Seven RWI data sets corresponding to seven provinces (Sitka, Peril Strait, North and South Prince of Wales, Mitkof Island, Kupreanof Island, and Point Nemo) were analyzed in seven identical climate–growth models using the Ketchikan–Annette weather record, which was chosen because it had the fewest gaps. Monthly temperature and precipitation indices in the models included a 12 month period from September of the current year (t) to the September of the previous year (t – 1). The stepwise procedure entered significant variables (i.e., monthly indices) into the model at the $p < 0.1$ level. Parameter estimates and significance of explanatory variables were compared across models to determine the monthly indices that were the best predictors of interannual variation in yellow-cedar RWI. We used these insights mainly to understand the importance of winter climate on cedar growth relative to other times of the year, i.e., during the hypothesized period where thaw–freeze injury may occur (February–April). Pearson correlation analyses (pairwise comparisons of monthly climate indices and RWI data sets) were used to confirm the accuracy of inferences drawn from the multivariate model outputs.

Results

Winter climate change in southeastern Alaska

Warming trends in the late winter (January–April) were observed in the 20th century instrumental records in the Ketchikan and Wrangell–Petersburg locales, but not in Sitka (Table 2). Ketchikan–Annette records indicated the strongest warming trends in the region and are depicted in Fig. 2. Warming trends were of lesser magnitude in the Wrangell–Petersburg combined record; only February and March warming trends were significant at $p < 0.01$. Overall, these results indicated that February temperature increases have been of the largest magnitude, relative to the other late-winter months. Although negative trends were observed in Sitka (with the exception of January MMT), none of the Sitka MMT regression models were significant ($p > 0.05$).

Based on linear regression models of sea level measurements, mean winter snowfall in southeastern Alaska has declined by 21.2 mm/year since 1950. Snowfall records indicated an approximate 20 year periodicity that has steadily trended downward since 1950 (Fig. 3). If extrapolated over the 20th century, this trend indicates an overall snowfall decrease of >2 m (at sea level) since 1900. Yet because of its decadal periodicity, mean winter snowfall tends to be highly variable from year to year. For example, based on Juneau records, four of the five lowest snowfall winters have occurred in the last 15 years, but the highest snowfall on record occurred in the most recent winter of 2006–2007 (which is not depicted in Fig. 3). Meanwhile, late-winter (January-April) rainfall has trended upward by 6.2 mm/year during the 20th century (Fig. 3), suggesting that an increasing proportion of winter precipitation is occurring as rain instead of snow, at elevations near sea level.

Frequency and magnitude of thaw–freeze events

The analysis of MDT records for four localities (Ketchikan-Annette, Sitka, Wrangell, and Petersburg) identified two sets of potential thaw–freeze events based on two criteria: (*i*) 3 GD, 1 FD and (*ii*) 7 GD, 3 FD. From 1902 to 2004, there were 17 years for which the minimal criteria of 3GD, 1FD were not found in any weather record during the period of 1 February – 30 April. The remaining 85 years composed the "baseline population" that estimated an upper bound for thaw–freeze frequency. No significant trend in frequency was observed in this set of events. These 3GD, 1FD events were regularly observed at more than one weather station; on average, each thaw–freeze event was found in 56.5% of the available records in a given year. Among the weather records, the highest frequency of 3GD, 1FD was found in Sitka ($n = 62$), and the lowest frequency was found in Petersburg ($n = 52$). Thaw–freeze frequency estimates used for station comparisons were based on the concurrent recording period (1920–2004).

For the lower bound estimate of thaw–freeze frequency, we identified 21 years where at least seven growing days preceded at least three freezing days (i.e., 7GD, 3FD) in February–April. Sitka records contained the highest frequency of these long-duration events ($n = 9$), and Wrangell was the lowest ($n = 5$). Fifteen of these events were after 1950, and seven have occurred since 1987. Only five of these events were observed in more than one record simultaneously, and only one (of these five) occurred prior to 1978. The only 7GD, 3FD thaw–freeze observed in all weather records during the 20th century occurred in 1987 (Fig. 4).

Fig. 3. Regional trends in mean winter snowfall (October–April) and mean late-winter rainfall (January–April) in southeastern Alaska based on existing weather records for the 20th century. Solid lines are linear regression fits with 95% confidence intervals (light dotted lines). Broken lines are cubic spline fits used for illustrative purposes.

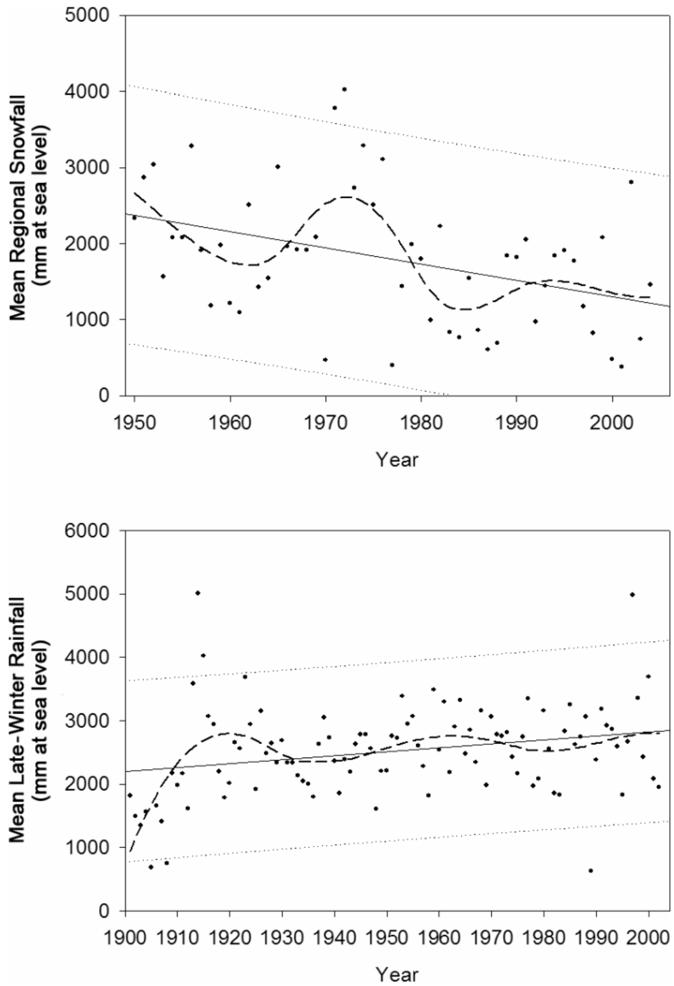

The values of M_{tf} were estimated by calculating the warming intensity during thaws (cumulative GDD >5 °C MDT) and freezing intensity following thaws (cumulative CDD <0 °C MDT) and summing these parameters for each year a thaw–freeze event was observed, for each of the four weather records. Mean GDD and CDD of thaw–freeze events varied among weather stations: Ketchikan–Annette had the highest mean GDD and the lowest mean CDD (warmer thaws and milder frosts); conversely, Petersburg had the lowest mean GDD and highest mean CDD (milder thaws and colder frosts). Mean M_{tf} did not significantly vary among weather records (two-sided *t* test, $p > 0.05$) but was highest in Wrangell (43.03) and lowest in Sitka (38.21). We ranked each year by magnitude, based on mean regional M_{tf} aggregated from all weather records, and found that 5 of the top 10 years of thaw–freeze magnitude have occurred

Fig. 4. The 1987 thaw–freeze event based on mean daily temperatures from four weather records. After a prolonged thaw, temperatures dropped approximately 10 °C in 4 days and remained below freezing for 7–10 days, depending on the weather record. Growing (5 °C) and freezing (0 °C) reference temperatures are depicted as horizontal broken lines.

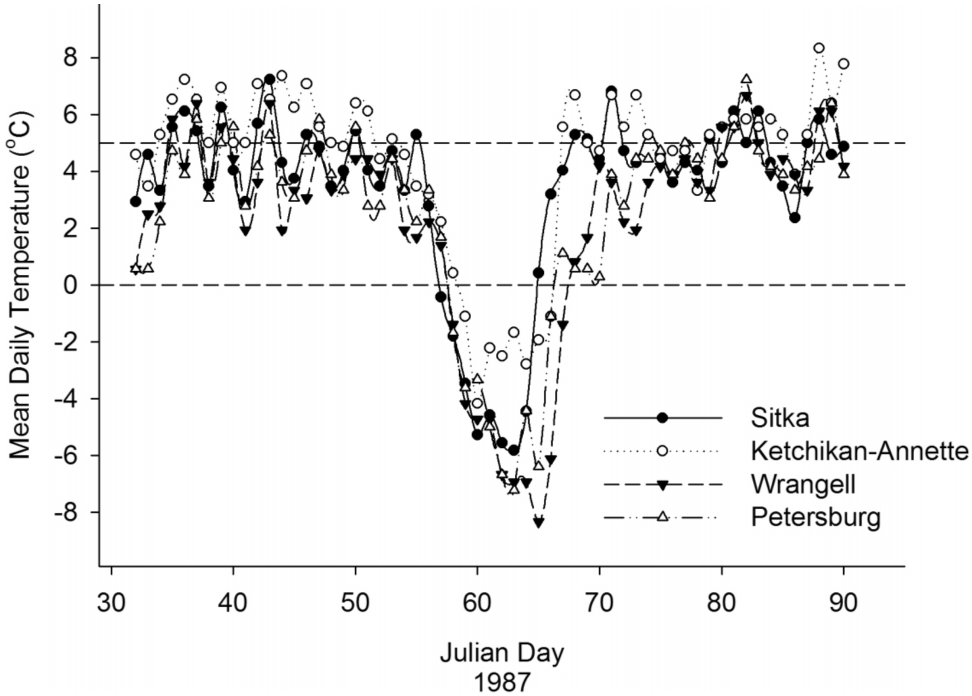

Table 3. Ten highest ranked winters of thaw–freeze magnitude from 1920 to 2004 based on the sum of mean regional growing degree-days (GDD ≥ 5 °C) prior to frost and mean cooling degree-days postthaw (CDD ≤ 0 °C) from February to April of each year.

Year	Thaw GDD	Freeze CDD	Magnitude rank
1954	14.50	103.31	1
1987	28.81	74.75	2
1996	39.13	61.50	3
2003	20.83	70.08	4
1917	5.00	83.00	5
1921	22.50	58.25	6
2001	10.13	61.56	7
1995	24.31	46.06	8
1956	3.63	65.13	9
1941	21.63	44.25	10

Note: The years refer to the winter season continuing from the previous year (e.g., 1954 represents the 1953–1954 winter).

Table 4. Ten highest ranked winters of potential thaw–freeze impact from 1950 to 2004 based on thaw–freeze magnitude and a proxy for snow cover (see eq. 1 in Methods).

Year	Magnitude	Snow cover	Impact rank
1987	103.56	–1.35	1
2001	71.69	–1.61	2
2003	90.92	–1.20	3
1986	53.81	–1.06	4
1997	64.75	–0.71	5
1970	25.50	–1.51	6
1992	36.38	–0.93	7
1988	22.31	–1.25	8
1993	59.88	–0.40	9
1983	18.81	–1.09	10

Note: The years refer to the winter season continuing from the previous year (e.g., 1987 represents the 1986–1987 winter).

since 1987 (Table 3). However, no significant trend in mean magnitude was found during the concurrent period of record ($p > 0.05$).

By combining estimates of thaw–freeze magnitude with a proxy for snow cover, we identified the highest ranking years where weather conditions best matched the suite of factors that we hypothesized were proximate with cedar injury and mortality. From 1950–2004, nine of the top 10 years of thaw–freeze impact (*I*) have occurred since 1983 (Table 4). For each of these years, uncommonly warm thaws and hard freezes occurred during winters in which snowfall (at elevations near sea level) was relatively low. The highest-ranked year was 1987, when the fifth-lowest snowfall year on record coincided with the only long-duration [7GD, 3FD] event observed in all weather records (Fig. 4).

Yellow-cedar population structure and growth chronologies

Prior studies on yellow-cedar decline have suggested that low-elevation cedar stands were established earlier than 1900 (Hennon and Shaw 1994). Our results verify that, at a landscape scale, the extant low-elevation yellow-cedar populations that are currently experiencing decline were established during the LIA. Nearly all trees in the sample population were dated prior to 1880 with an estimated mean age of 236 years (1768–2004). This is definitely a low estimate of mean age, because accurate cross-dating was not

Table 5. Pearson *r* correlations among tree-ring chronologies of yellow-cedar in declining populations by province from 1900 to 2004.

	Mitkof	Kupreanof	Wrangell	Sitka	Peril Strait	Northern POW	Southern POW	Poison Cove Bog
Kupreanof	0.67***							
Wrangell	0.72***	0.69***						
Sitka	0.68***	0.56***	0.54***					
Peril Strait	0.72***	0.61***	0.78***	0.8***				
Northern POW	0.66***	0.78***	0.57***	0.53***	0.59***			
Southern POW	0.51***	0.57***	0.51***	0.47***	0.58***	0.79***		
Poison Cove Bog	0.28***	0.42***	0.4***	0.08	0.38***	0.48***	0.53***	
Juneau	–0.11	–0.11	–0.14	–0.37***	–0.33***	0.01	0.18	0.44***

Note: Two healthy populations (Poison Cove Bog and Juneau) are included for reference. Significant Pearson *r* correlations ($p < 0.0001$) are indicated with asterisks. POW, Prince of Wales Island.

possible prior to 1700 in many cases, as a result of either missing rings or the use of partial cores on very large trees. We also cored yellow-cedar snags in several decline sites that were impossible to cross-date (because of decay) but that typically had several hundred rings. Less than 5% of the sample population dated prior to 1400.

At the regional scale, declining yellow-cedar populations shared a common growth signal from 1900 to 2004 based on correlation analysis of aggregated mean chronologies (Table 5). Marker years of exceptionally low growth were found in nearly all tree-ring series (from declining populations) for 1912, 1936, 1957, 1958, and 1987 (Fig. 5). Mean radial growth and interannual variability (in growth) has trended upward for declining, low-elevation cedar forests since the end of the LIA. In other words, surviving trees in declining forests have produced generally larger rings but with approximately twice the interannual variability since the onset of decline. When normalized chronologies were partitioned by century, mean RWI variance was significantly higher during the 20th century compared with the 19th century (two sided F test, $p < 0.0001$). Annual growth of the healthy Juneau population was unrelated or negatively correlated with declining populations (Table 5) and exhibited a significantly higher mean variance during the 19th century than the 20th century (two sided F test, $p < 0.0001$), a trend opposite of that observed for declining populations. With the exception of 1958, ring series from the healthy Juneau population did not share the same marker years found in declining populations.

Climatic influences on cedar growth

According to multivariate models and pairwise correlation analyses, early winter (October–December) and late-winter (March–April) climate have exerted the strongest landscape-scale influences on growth of surviving trees in declining cedar populations. The best climatic predictors of declining cedar RWI in multivariate models, and verified by correlation analysis, are given in Table 6. For healthy cedar RWI, based on the Juneau site, the best climatic predictors centered on growing season conditions, i.e., summer (May–August) temperature and precipitation.

During the 19th century, annual growth of the low-elevation and high-elevation cedar populations in the Poison Cove watershed were strongly correlated ($r = 0.63$, $p < 0.0001$), indicating a common growth pattern within the watershed (Fig. 6*a*). This correlation was weakly significant for the 20th century ($r = 0.21$, $p < 0.01$), indicating some decoupling of the shared growth signal of the two populations (Fig. 6*b*). Also, climate–growth relationships for the two sites differed during the 20th century. Growth models indicated the importance of late-winter weather at the low-elevation site, where cedar is dying, and the importance of growing season conditions at the high-elevation site, where cedar does not suffer from decline symptoms. However, both Poison Cove chronologies shared marker years during the 20th century, including 1912, 1957, and 1987 (Fig. 6*c*).

Discussion

Overall, we found several lines of evidence that validated the assumptions of our working hypothesis of cedar decline as an emergent phenomenon driven by climate change. During the period of instrument record, winter climate in southeastern Alaska has warmed, resulting in a suite of conditions consistent with our cedar-decline hypothesis, i.e., early thaws, subsequent freezes, and low snow cover. Although warming has apparently driven an increase in the frequency and magnitude of early thaws, the occurrence of freezing conditions has remained consistent during the 20th century. This initially perplexing observation can be explained by the characteristic "bivalence" of southeastern Alaska weather, which tends to occur by one of two types of systems: (*i*) a low pressure maritime front, which is the most common and persistent condition throughout the year, or (*ii*) a high pressure front originating in the arctic mainland that brings clear and sunny conditions. During the winter, the maritime low generates mild temperatures and nearly constant precipitation, whereas the arctic high pressure brings freezing conditions that can persist for a week or longer. These transitions to frost conditions occur rapidly and have been typical of regional weather patterns in southeastern Alaska; however in recent decades, they have increasingly been preceded by warmer and earlier thaws, often in conjunction with low snowfall at low elevations. We found that thaw–freeze events occurred regularly during the 20th century, especially in the latter half. Because of declining snowfall resulting in reduced snow cover, the majority of potentially injurious thaw–freeze events have occurred in the last two decades, although this observation has limited validity for the 20th century because of the lack of snowfall data before 1950. Moreover, our observations of thaw–freeze occurrence in February and March are

Fig. 5. Comparison of 1800–2004 standardized growth chronologies (ring width indices, RWI) for four region-aggregated declining cedar populations and one healthy cedar population (Juneau). Increasing overall growth in declining populations during the 20th century may be attributable to competitive release caused by decline-related mortality in the stand.

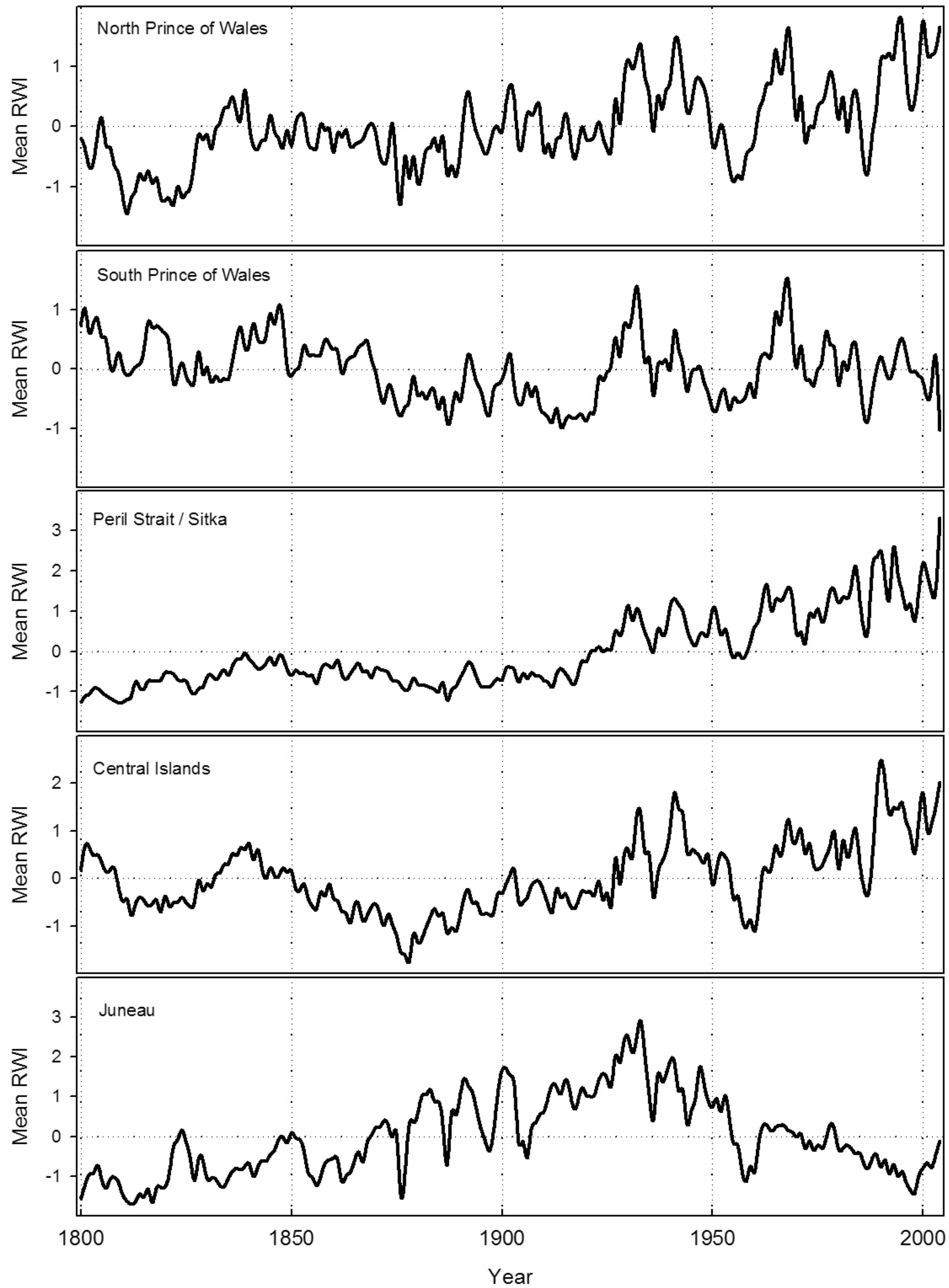

consistent with recent experimental findings confirming that cedar is capable of dehardening as early as February (Schaberg et al. 2008) and that foliar injury is visually apparent in late March – early April (P.E Hennon, unpublished data).

Growth patterns and climate sensitivity of yellow-cedar in southeastern Alaska were also consistent with our hypothesis. Declining cedar populations across the region shared a common growth signal, which has responded to late-winter climate more strongly and consistently than any other time of year, including the growing season. Since the onset of the decline phenomenon ca. 1900, we observed that (*i*) healthy populations have not shared this growth signal with declining populations, (*ii*) healthy populations responded differently to climatic variation, and (*iii*) declining populations have experienced both increased growth and greater interannual variability in growth. Increased growth may be due to several factors, including overall warmer temperatures resulting in longer growing seasons (Barber et al. 2000), as well as the effects of competitive release on growth of surviving trees (Antos and Parish 2002). Increased variability in growth may also be the result of greater fre-

Table 6. Components of multivariate climate models that best predicted cedar growth in declining stands during 1900–2004.

Model type and month (of seven models)	Frequency	Effect
MMT		
May	3	Positive
April	5	Positive
March	6	Positive
January	3	Negative
November (*t* – 1)	3	Positive
MPPT		
April	7	Negative
December (*t* – 1)	4	Positive
November (*t* – 1)	4	Negative
October (*t* – 1)	6	Negative

Note: Seven models were built based on grouped (by province) cedar chronologies, and only those variables present in at least three models are shown. Values in parentheses indicate that the data were from the prior year. MMT, mean monthly temperature; MPPT, total monthly precipitation.

quency of proximate stressors (Apple and Manion 1986; Fritts 1990).

The suite of environmental stressors postulated by our hypothesis were best represented in the winters of 1985–1986 and 1986–1987; these years ranked fourth and first, respectively, in estimated thaw–freeze impact (based on thaw–freeze magnitude and relative snow cover) among all years from 1950 to 2004. During these two consecutive winters, our findings suggest that low-elevation yellow-cedar forests were highly susceptible to climatic stressors because of prolonged, high-intensity thaw–freeze events in conjunction with low snowfall. Given these conditions, our hypothesis would predict that cedar trees suffered extensive root mortality that either resulted in crown death and rapid senescence (Hennon et al. 2006) or stunted growth for surviving trees. Although our tree ring records were based solely on surviving trees, there is dendrochronological evidence for both a stress response and a pulse of mortality. Nearly all ring series contained marker years of exceptionally low growth for 1986 and 1987. All decline site chronologies increased sharply after 1987, an observation that may be explained, in part, by the competitive release of surviving trees. Age-class studies of cedar snags indicated that a pulse of mortality occurred around this time (Hennon et al. 1990). More broadly, when we compared thaw–freeze magnitude to declining cedar chronologies during the 20th century (Fig. 7), we found that certain periods of putative climatic stress have coincided with periods of depressed growth; e.g., 1940–1945, 1954–1956, 1986–1987, and 1995–1997. Although we cannot definitively establish causation from this evidence, it is highly consistent with our decline hypothesis across large spatial and temporal scales.

Yellow-cedar is healthy in the high-elevation habitat common throughout its range, whereas the decline condition is found almost entirely at low elevations in southeastern Alaska and northern British Columbia. Yet, we found that, in our paired sites at Poison Cove, the high-elevation healthy site appeared to be equally (and possibly more) sensitive to the proximate stressors that resulted in the marker years of 1986 and 1987. If these stressors were associated with thaw–freeze events, as they appeared to be in 1986 and 1987, then why are symptoms of decline absent at high elevations in Poison Cove? We suggest that high-elevation cedar benefits from a colder microclimate, and several lines of evidence support this hypothesis. Firstly, adiabatic lapse rates of temperature with elevation in southeastern Alaska are estimated to be 0.55 °C/100 m (see Viens 2001), meaning that ambient temperatures in healthy cedar stands near timberline may be between 3 and 7 °C colder than stands near sea level. As a result, thaw frequency and severity decreases with elevation, an observation verified by comparisons of winter air temperatures across sites at Poison Cove (D'Amore and Hennon 2006). Secondly, the likelihood of premature dehardening in yellow-cedar is lessened at higher elevations, and therefore, cedar at high elevations retains cold hardiness throughout cycles of thawing and freezing occurring at lower elevations. A recent study found that, when sampling of foliage was conducted in April at the Poison Cove sites, cedar trees growing below 130 m were less cold hardy than those growing above 130 m (Schaberg et al. 2005). Thirdly, compared with sites near sea level, yellow-cedar stands at higher elevations experience greater snow accumulation and longer persistence of snow cover into the growing season (D'Amore and Hennon 2006). Persistent insulative snowpack may mitigate against temperature fluctuations that both initiate dehardening in shallow roots (via soil thawing) and cause freezing injury (via soil refreezing). Thus, although thaw–freeze events may damage dehardened foliar tissues, cedar remains healthy where snow cover remains adequate to insulate soils and roots.

Landscape-scale observations further support the role of snow cover in the cedar decline mechanism. Based on a recently developed landscape model of snow accumulation in southeastern Alaska (D. Albert, The Nature Conservancy, Juneau, Alaska, unpublished data), we estimated the total acreage of observed cedar decline (based on Wittwer 2004) in each of the four snowfall zones produced by the model, e.g., low, moderate, high, and very high. Using this coarse-resolution approach, we found that the vast majority (78.8%) of declining cedar stands were located in low snow zones (Fig. 8), and nearly all (94.3%) were found in either low or moderate zones.

The temperature-dependent spring physiology of yellow-cedar may explain why sympatric species in southeastern Alaska are not experiencing similar decline in response to thaw–freeze events (Silim and Lavender 1994). Between winter and spring measurements, yellow-cedar dehardens up to 13 °C more than the sympatric western hemlock, making it far more vulnerable to freezing injury in the late winter (Schaberg et al. 2005). Because it exhibits indeterminate growth, yellow-cedar is capable of shoot elongation prior to the budbreak of competing species (Puttonen and Arnott 1994). This adaptation likely provided a competitive advantage during the LIA, allowing the slow-growing cedar to compete with faster growing Sitka spruce and western hemlock (Hebda 1983; Carrarra et al. 2003). With a shift to a warming climate, there is substantial evidence that this trait has become a vulnerability for low-elevation yellow-cedar,

Fig. 6. Statistical and qualitative comparisons of cedar growth chronologies (ring width indices, RWI) between paired sites in the Poison Cove watershed indicating that a common growth signal during the 19th century was decoupled during the 20th century. Analysis is based on a linear model partitioned by century, providing two regressions: (*a*) 1800–1899 and (*b*) 1900–1999. Regressions are plotted with 95% confidence intervals. (*c*) Chronologies plotted in parallel from 1800 to 2004.

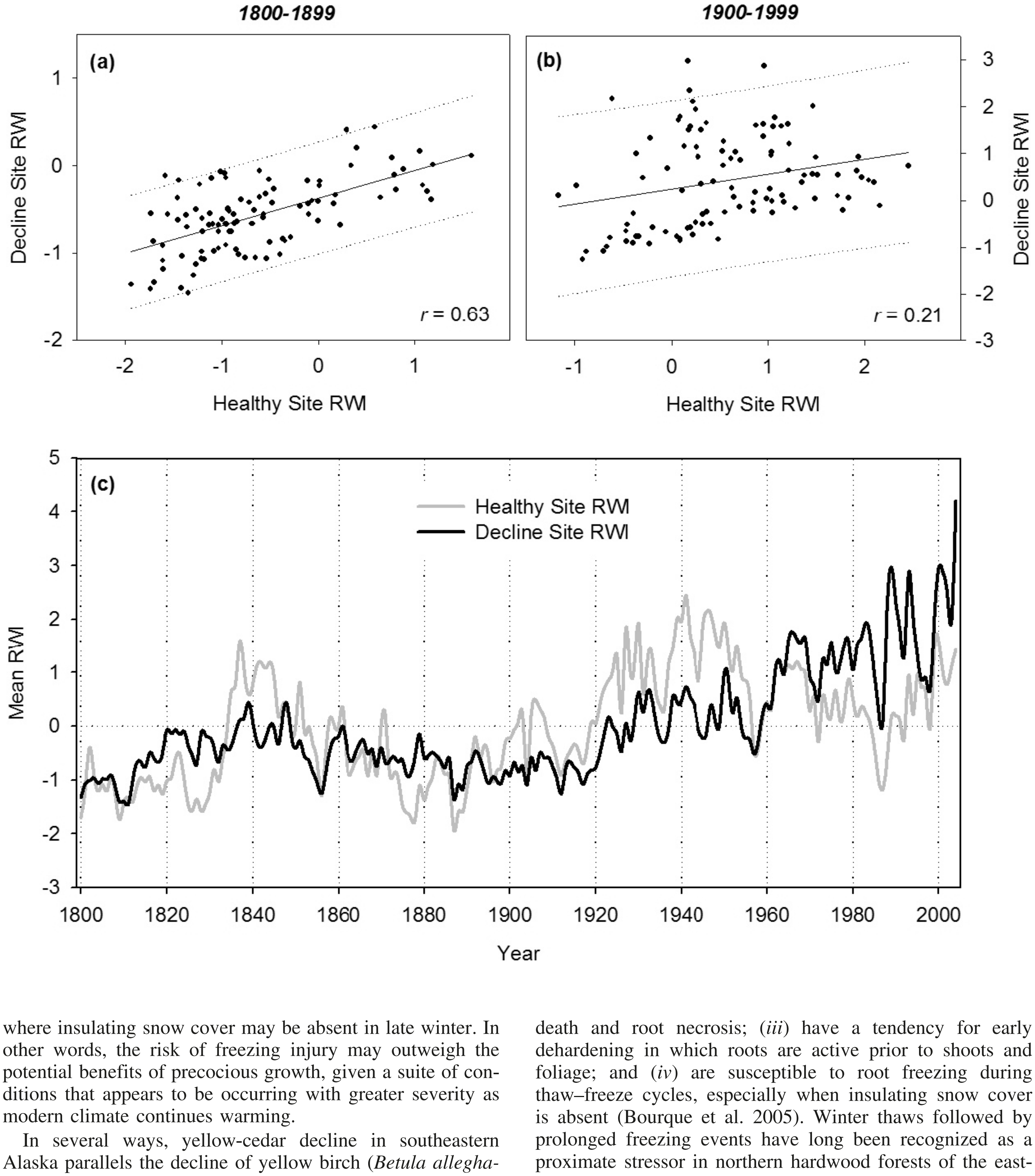

where insulating snow cover may be absent in late winter. In other words, the risk of freezing injury may outweigh the potential benefits of precocious growth, given a suite of conditions that appears to be occurring with greater severity as modern climate continues warming.

In several ways, yellow-cedar decline in southeastern Alaska parallels the decline of yellow birch (*Betula alleghaniensis* Britt.) in northeastern North America. Both species are (*i*) limited to high elevations in the southern areas of their range; (*ii*) have declining populations in the northern areas of their range, with similar symptoms involving crown death and root necrosis; (*iii*) have a tendency for early dehardening in which roots are active prior to shoots and foliage; and (*iv*) are susceptible to root freezing during thaw–freeze cycles, especially when insulating snow cover is absent (Bourque et al. 2005). Winter thaws followed by prolonged freezing events have long been recognized as a proximate stressor in northern hardwood forests of the eastern United States and Canada (Auclair et al. 1996, 1997). Thaw–freeze cycles have been linked with xylem cavitation, freezing of dehardened shallow roots, and shoot dieback in yellow birch; all are proximate factors in the decline of the

Fig. 7. Comparison of thaw–freeze magnitude and growth chronologies (ring width indices, RWI) for declining yellow-cedar populations in southeastern Alaska. Mean cumulative growing degree-days (GDD) prior to frost are plotted as shaded bars, and mean cumulative cooling degree-days (CDD) after the thaw are plotted as solid bars. CDD are given negative values in this figure for illustrative purposes only. Standardized cedar chronologies are plotted in parallel with thaw–freeze records from 1910 to 2004.

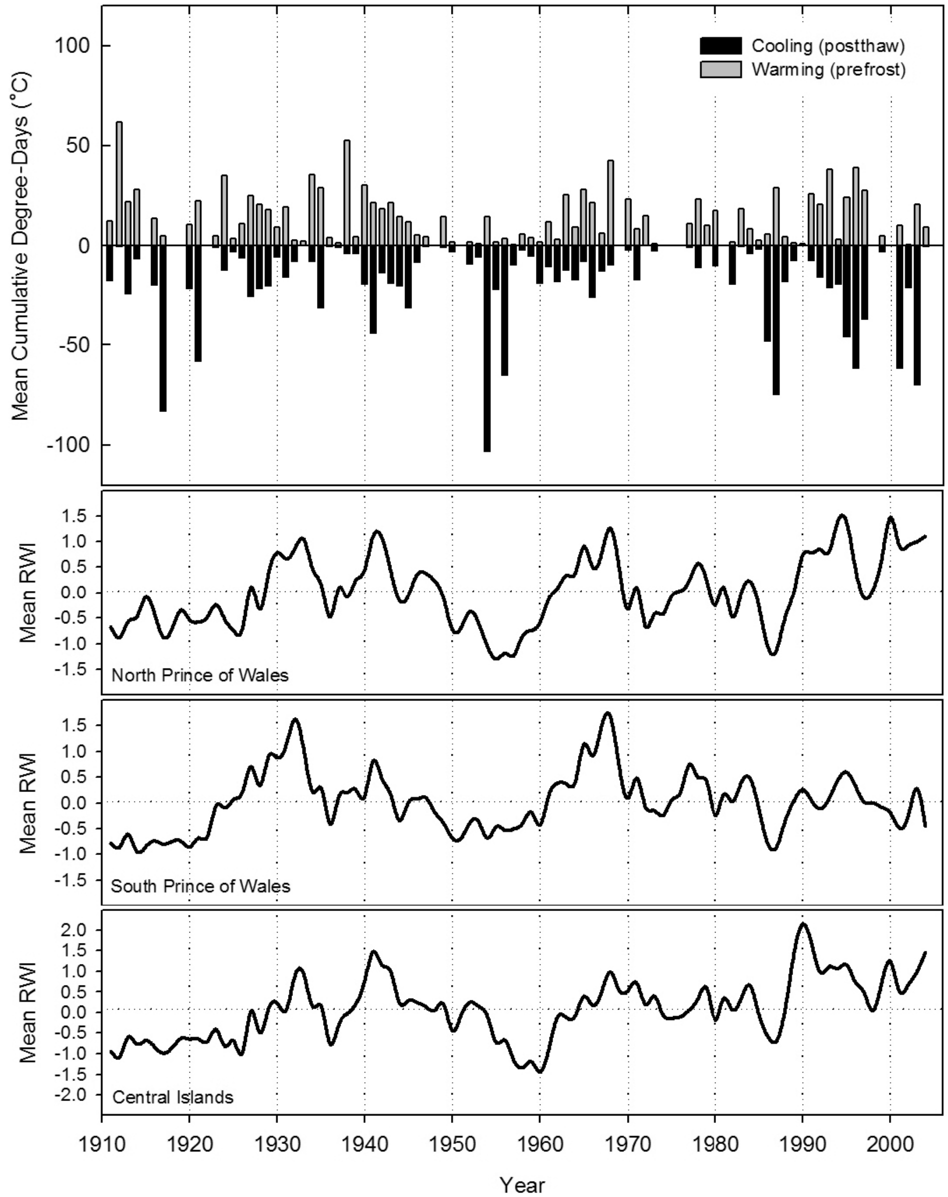

species (Zhu et al. 2001, 2002). Despite these similarities, establishing the role of climatic stressors in yellow-cedar dieback in Alaska and Canada requires further physiological and experimental research in the vein of recent work by Schaberg et al. (2005, 2008) and D'Amore and Hennon (2006). Our current findings provide a broader justification of these future efforts, especially considering that they will likely require considerable investments to conduct snow cover manipulations, microclimatic monitoring, and in situ observations of belowground tree injury, among other measures needed to elucidate the mechanism(s) of decline.

In closing, it appears that recent warming in the hyper-maritime climate of southeastern Alaska has generated a complex suite of conditions for yellow-cedar that has both supported increased average growth (that may be due to warmer growing season temperatures and (or) the effects of competitive release on surviving trees), and driven episodic mortality events at landscape scales, as evidenced most dramatically in the winters of 1986 and 1987. If current trends continue, cedar dieback may expand upslope into currently healthy populations, raising concern for scientists and resource managers interested in maintaining this long-lived and valuable species in the coastal rainforests of Alaska and British Columbia; in fact, upslope expansion of decline sites has already been observed in several areas in

Fig. 8. Comparison of areas of low snow accumulation (left map, solid areas) and the occurrence of cedar decline (right map, solid areas) across southeastern Alaska. Snow map based on PRISM model estimates of snow accumulation categorized into low, moderate, high, and very high zones; only the low zone is shown on map (D. Albert, The Nature Conservancy, Juneau, Alaska, unpublished data). The cedar decline map is based on aerial survey data (Wittwer 2004).

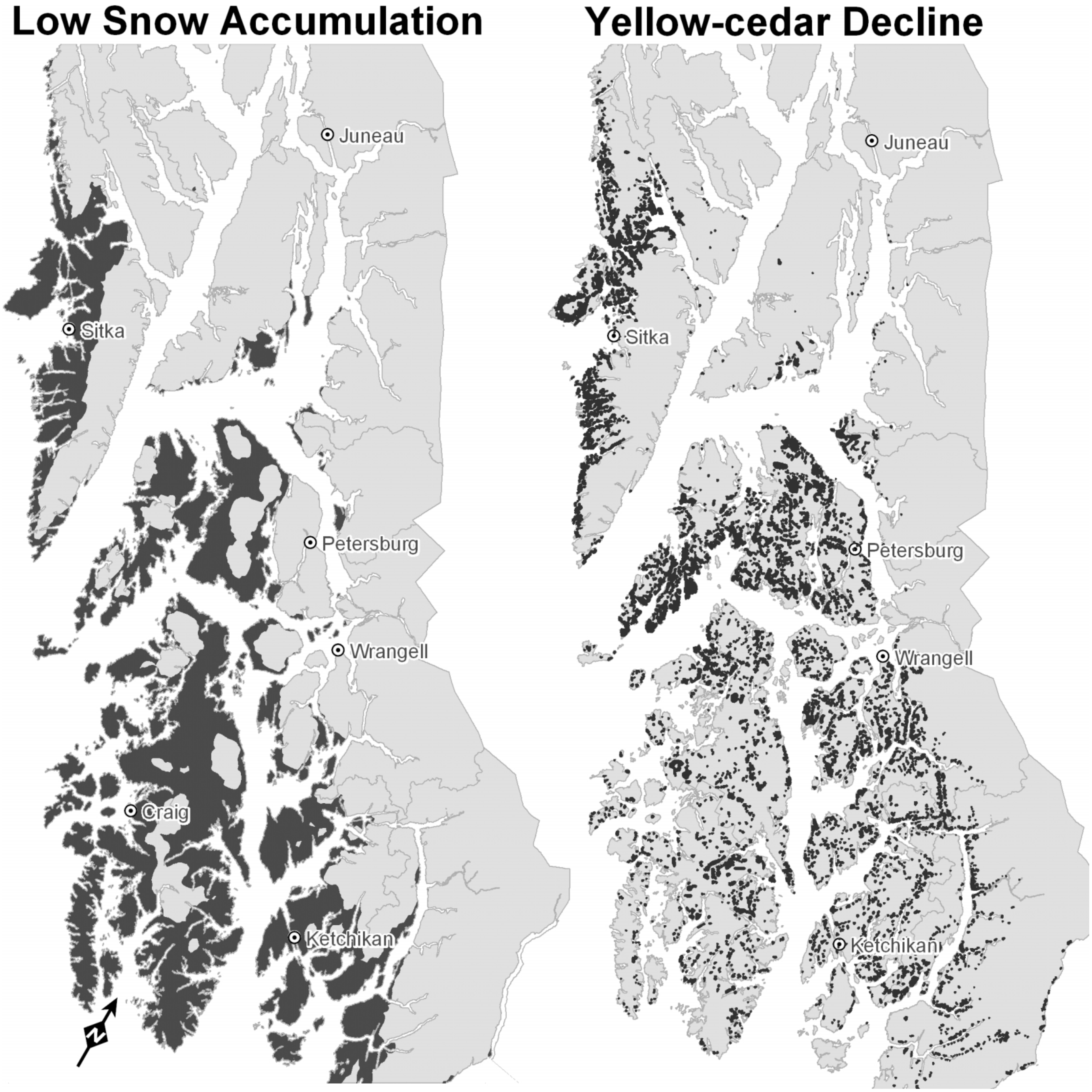

southeastern Alaska (Hennon et al. 2006). More broadly, our findings suggest the vulnerability of temperate rainforests to global change. Cedar decline may be a harbinger of future ecological changes in this globally rare and unique biome.

Acknowledgements

We thank Terry Chapin and Dave McGuire (University of Alaska Fairbanks) for support in acquiring supplies and providing manuscript reviews, Dave Albert (The Nature Conservancy) for providing the snow accumulation model, and the Juneau Forestry Sciences Laboratory (USDA Forest Service Pacific Northwest Research Station) for logistical support. Thanks to Kake Tribal Corporation and Haida Corporation for allowing us to conduct field work on their private inholdings. Funding for this study was provided by USDA New Crops and the University of Alaska Fairbanks Center for Global Change.

References

Alaska Climate Research Center (ACRC). 2007. Temperature change in Alaska. [online] ACRC, University of Alaska, Fairbanks, Alaska.http://climate.gi.alaska.edu/ClimTrends/Change/TempChange.html

Antos, J.A., and Parish, R. 2002. Dynamics of an old-growth, fire-initiated, subalpine forest in southern interior British Columbia: tree size, age, and spatial structure. Can. J. For. Res. **32**: 1935–1946. doi:10.1139/x02-116.

Apple, J.D., and Manion, P.D. 1986. Increment core analysis of declining Norway maples, *Acer platanoides*. Urban Ecol. **9**: 309–321. doi:10.1016/0304-4009(86)90006-9.

Auclair, A.N.D., Lill, J.T., and Revenga, C. 1996. The role of climate variability and global warming in the dieback of northern hardwoods. Water Air Soil Pollut. **91**: 163–186. doi:10.1007/BF00666255.

Auclair, A.N.D., Eglinton, P.D., and Minnemeyer, S.L. 1997. Principal forest dieback episodes in northern hardwoods: development of numeric indices of area extent and severity. Water Air Soil Pollut. **93**: 175–198. doi:10.1007/BF02404755.

Barber, V.A., Juday, G.P., and Finney, B.P. 2000. Reduced growth of Alaskan white spruce in the twentieth century from temperature-induced drought stress. Nature (Lond.), **405**: 668–673. doi:10.1038/35015049. PMID:10864320.

Bourque, C.-P.A., Cox, R.M., and Allen, D.J. 2005. Spatial extent of winter thaw events in eastern North America: historical weather records in relation to yellow birch decline. Glob. Change Biol. **11**: 1477–1492. doi:10.1111/j.1365-2486.2005.00956.x.

Carrarra, P.E., Ager, T.A., and Baichtal, J.F. 2003. Map of glacial limits and possible refugia in the southern Alexander Archipelago, Alaska, during the late Wisconsin glaciation. US Geological Survey, Washington, D.C. USGS Misc. Field Stud. Map MF-2424.

Cook, E.R., and Krusic, P.J. 2005. Program ARSTAN: a tree-ring standardization program based on detrending and autoregressive time series modeling. Tree Ring Laboratory, Lamont Doherty Earth Obsservatory, Columbia University, New York.

D'Amore, D.V., and Hennon, P.E. 2006. Evaluation of soil saturation, soil chemistry, and early spring soil and air temperatures as risk factors in yellow-cedar decline. Glob. Change Biol. **12**: 524–545. doi:10.1111/j.1365-2486.2006.01101.x.

Fritts, H.C. 1990. Modeling tree-ring and environmental relationships for dendrochronological analysis. *In* Process modeling of forest growth responses to environmental stress. *Edited by* R. Dixon, R. Meldahl, G. Ruark, and W. Warren. Timber Press, Portland, Ore. pp. 368–382.

Harris, A.S. 1990. *Chamaecyparis nootkatensis* (D. Don) Spach: Alaska-cedar. *In* Silvics of North America. Vol. 1. Conifers. *Technical coordinators*: R.M. Burns and B.H. Honkala. US Dep. Agric. Agric. Handb. 654. pp. 97–102.

Havranek, W.M., and Tranquillini, W. 1995. Physiological processes during winter dormancy and their ecological significance. *In* Ecophysiology of coniferous forests. *Edited by* J. Roy, W. Smith, and T. Hinckley. Academic Press, New York. pp. 95–124.

Hawkins, B.J., Russel, J.H., and Arnott, J.T. 2001. Cold hardiness of yellow-cedar (*Chamaecyparis nootkatensis* (D. Don) Spach). *In* Conifer cold hardiness. *Edited by* F.J. Bigras and S.J.. Colombo. Kluwer Academic Publishers, Dordrecht, the Netherlands. pp. 531–554.

Hebda, R.J. 1983. Late-glacial and postglacial vegetation history at Bear Cove Bog, northeast Vancouver Island, British Columbia. Can. J. Bot. **61**: 3172–3192. doi:10.1139/b83-355.

Hennon, P.E., and Shaw, C.G. 1994. Did climatic warming trigger the onset and development of yellow-cedar decline in southeast Alaska? Eur. J. For. Pathol. **24**: 399–418. doi:10.1111/j.1439-0329.1994.tb00833.x.

Hennon, P.E., and Shaw, C.G. 1997. The enigma of yellow-cedar decline: what is killing these long-lived, defensive trees? J. For. **95**: 4–10.

Hennon, P.E., Shaw, C.G., and Hansen, E.M. 1990. Dating decline and mortality of *Chamaecyparis nootkatensis* in southeast Alaska. For. Sci. **36**: 502–515.

Hennon, P.E., D'Amore, D.V., Zeglen, S., and Granger, M. 2005. Yellow-cedar decline in the North Coast Forest District of British Columbia. USDA For. Ser. Pac. Northwest Res. Stn. Res. Note RN-549.

Hennon, P.E., D'Amore, D.V., Wittwer, D., Johnson, A., Schaberg, P., Hawley, G., Beier, C., Sink, S., and Juday, G. 2006. Climate warming, reduced snow, and freezing injury could explain the demise of yellow-cedar in southeast Alaska, USA. World Resour. Rev. **18**: 427–450.

Heusser, C.J., Heusser, L.E., and Peteet, D.M. 1985. Late-Quaternary climatic change on the American North Pacific coast. Nature (Lond.), **315**: 485–487. doi:10.1038/315485a0.

Holmes, R.L. 1983. Computer assisted quality control in tree-ring dating and measurement. Tree-Ring Bull. **43**: 69–75.

Juday, G.P. 1984. Temperature trends in the Alaska climate record. *In* Proceedings of the Conference on the Potential Effects of Carbon Dioxide-Induced Climatic Changes in. Alaska, 7 Apr. 1982, Fairbanks, Alaska. *Edited by* J.H. McBeath. University of Alaska, Fairbanks, Alaska. Univ. Alaska Agric. Exp. Stn. Misc. Publ. 83-1. pp. 76–88.

Laroque, C.P., and Smith, D.J. 1999. Tree ring analysis of yellow-cedar (*Chamaecyparis nootkatensis*) on Vancouver Island, British Columbia. Can. J. For. Res. **29**: 115–123. doi:10.1139/cjfr-29-1-115.

Neiland, B.J. 1971. The forest–bog complex in Southeast Alaska. Vegetatio, **22**: 1–63. doi:10.1007/BF01955719.

Puttonen, P., and Arnott, J.T. 1994. Influence of photoperiod and temperature on growth, gas exchange, and cold hardiness of yellow cypress stecklings. Can. J. For. Res. **24**: 1608–1616. doi:10.1139/x94-209.

Schaberg, P.G., Hennon, P.E., D'Amore, D.V., Hawley, G.J., and Borer, C.H. 2005. Seasonal differences in freezing tolerance of yellow-cedar and western hemlock trees at a site affected by yellow-cedar decline. Can. J. For. Res. **35**: 2065–2070. doi:10.1139/x05-131.

Schaberg, P.G., Hennon, P.E., D'Amore, D.V., and Hawley, G.J. 2008. Influence of simulated snow cover on the cold tolerance and freezing injury of yellow-cedar seedlings. Glob. Change Biol. In press.. doi:10.1111/j.1365-2486.2008.01582.x.

Silim, S.N., and Lavender, D.P. 1994. Seasonal patterns and environmental regulation of frost hardiness in shoots of seedlings of *Thuja plicata*, *Chamaecyparis nootkatensis*, and *Picea glauca*. Can. J. Bot. **72**: 309–316. doi:10.1139/b94-040.

Sperry, J.S., and Sullivan, J.E.M. 1992. Xylem embolism in response to freeze–thaw cycles and water stress in ring-porous, diffuse porous, and conifer species. Plant Physiol. **100**: 605–613. PMID:16653035.

Viens, R.J. 2001. Late Holocene climate change and calving glacier fluctuations along the southwestern margin of the Stikine Icefield, Alaska. Ph.D. dissertation, University of Washington, Seattle, Wash.

Viereck, L.A., and Little, E.L. 1986. Alaska trees and shrubs. University of Alaska Press, Fairbanks, Alaska.

Vincent, L.A., and Gullett, D.W. 1999. Canadian historical and homogeneous temperature datasets for climate change analysis.

Int. J. Climatol. **19**: 1375–1388. doi:10.1002/(SICI)1097-0088(199910)19:12<1375::AID-JOC427>3.0.CO;2-0.

Wittwer, D. 2004. Forest health conditions in Alaska. USDA For. Serv. Alaska Reg. Prot. Rep. R10-PR-3.

Zhu, X.B., Cox, R.M., and Meng, F.-R. 2001. Responses of xylem cavitation, freezing injury and shoot dieback to a simulated winter thaw in yellow birch seedlings growing in different nursery culture regimes. For. Ecol. Manage. **145**: 243–253. doi:10.1016/S0378-1127(00)00440-0.

Zhu, X.B., Cox, R.M., and Bourque, C.-P.A., and Arp, P.A. 2002. Thaw effects on cold-hardiness parameters in yellow birch. Can. J. Bot. **80**: 390–398. doi:10.1139/b02-022.